Wu, Yiyun; Gu, Baojing; Erisman, Jan Willem; Reis, Stefan; Fang, Yuanyuan; Lu, Xuehe; Zhang, Xiuming. 2016. **PM2.5 pollution is substantially affected by ammonia emissions in China**. *Environmental Pollution*, 218. 86-94. 10.1016/j.envpol.2016.08.027

$PM_{2.5}$ pollution is substantially affected by ammonia emissions in China

Yiyun Wu[1], Baojing Gu[1,2*], Jan Willem Erisman[3,4], Stefan Reis[5,6], Yuanyuan Fang[7], Xuehe Lu[8], Xiuming Zhang[1,9]

[1]Policy Simulation Laboratory, Zhejiang University, Hangzhou 310058, PR China
[2]Department of Land Management, Zhejiang University, Hangzhou 310058, PR China
[3]Louis Bolk Institute, Hoofdstraat 24, 3972 LA Driebergen, The Netherlands
[4]VU Amsterdam, De Boelelaan 1091, 1081 HV Amsterdam, The Netherlands
[5]NERC Centre for Ecology & Hydrology, Bush Estate, Penicuik, Midlothian, EH26 0QB, United Kingdom
[6]University of Exeter Medical School, Knowledge Spa, Truro, TR1 3HD, United Kingdom
[7]Deparment of Global Ecology, Carnegie Institution for Science, Stanford, 94305, CA, USA
[8]Jiangsu Provincial Key Laboratory of Geographic Information Science and Technology, International Institute for Earth System Science, Nanjing University, Nanjing 210023, China
[9]College of Life Sciences, Zhejiang University, Hangzhou 310058, PR China

***Corresponding Author:**
Department of Land Management, Zhejiang University, Zijingang Campus, 866 Yuhangtang Road, Hangzhou 310058, PR China. Tel & Fax: +86 571 8898 2615.
E-mail: bjgu@zju.edu.cn

Abstract

Urban air quality in China has been declining substantially in recent years due to severe haze episodes. The reduction of sulfur dioxide (SO_2) and nitrogen oxide (NO_x) emissions since 2013 does not yet appear to yield substantial benefits for haze mitigation. As the reductions of those key precursors to secondary aerosol formation appears not to sufficient, other crucial factors need to be considered for the design of effective air pollution control strategies. Here we argue that ammonia (NH_3) plays a - so far - underestimated role in the formation of secondary inorganic aerosols, a main component of urban fine particulate matter ($PM_{2.5}$) concentrations in China. By analyzing *in situ* concentration data observed in major cities alongside gridded emission data obtained from remote sensing and inventories, we find that emissions of NH_3 have a more robust association with the spatiotemporal variation of $PM_{2.5}$ levels than emissions of SO_2 and NO_x. As a consequence, we argue that urban $PM_{2.5}$ pollution in China in many locations is substantially affected by NH_3 emissions. We highlight that

more efforts should be directed to the reduction of NH_3 emissions that help mitigate $PM_{2.5}$ pollution more efficiently than other $PM_{2.5}$ precursors. Such efforts will yield substantial co-benefits by improving nitrogen use efficiency in farming systems. As a consequence, such integrated strategies would not only improve urban air quality, but also contribute to China's food-security goals, prevent further biodiversity loss, reduce greenhouse gas emissions and lead to economic savings.

A capsule:

$PM_{2.5}$ pollution in China is substantially affected by NH_3 emissions and more efforts should be directed to reducing NH_3 emissions to mitigate $PM_{2.5}$ pollution more efficiently.

Graphical Abstract

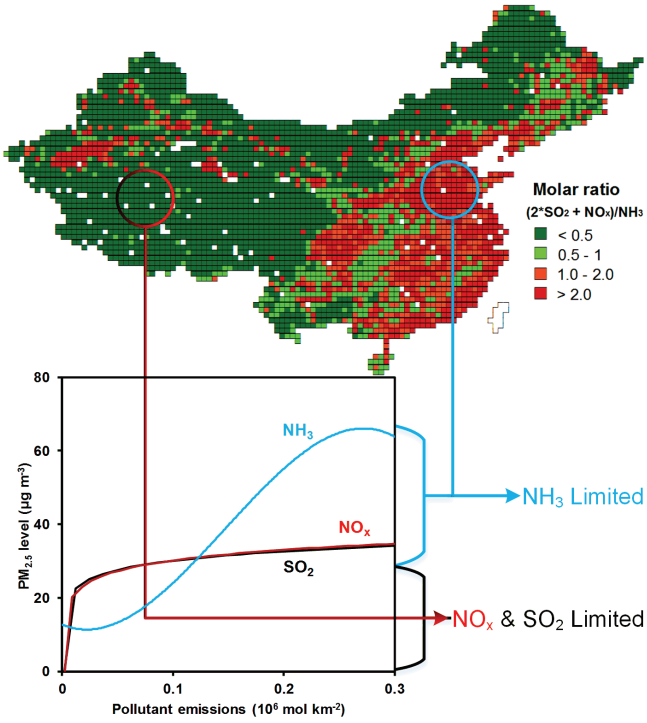

Key words: Ammonia emissions; Air pollution; Haze formation; Nitrogen; Panel model; Food security

1.Introduction

China experienced extremely severe and persistent haze episodes in recent years (Huang et al., 2014). The average annual $PM_{2.5}$ concentrations in 190 major cities do not meet the clean air standard for fine particulate matter recommended by the World Health Organisation (WHO, 10 μg m^{-3}), and the population-weighted mean of $PM_{2.5}$ concentrations in Chinese cities was 61 μg m^{-3}, approximately three times higher than

global population-weighted mean concentrations in 2014-2015 (Zhang and Cao, 2015). Severe haze in Northern China caused a loss of up to five life years on average, leading to a substantial detrimental effect on public health (Chen et al., 2013). To mitigate $PM_{2.5}$ pollution in China, the central government launched the "Clean Air Act" (CAA) and identified binding reduction targets for emissions of SO_2 and NO_x for each city (MEPC, 2016). Nevertheless, a recent study revealed significant increases, rather than decreases, in observed $PM_{2.5}$ concentrations in the years 2013 and 2014 as compared to 2012, when China's State Council set pollution reduction targets, excluding interannual variations due to meteorological factors (Liang et al., 2015). These findings suggest that emission reductions of SO_2 and NO_x do not present an effective approach to mitigate the $PM_{2.5}$ pollution. Thus, improving the understanding of the underlying processes for haze formation and identifying effective mitigation pathways are still unsolved challenges for China.

The most recent studies analysing $PM_{2.5}$ composition suggest that secondary inorganic aerosols (SIA, e.g., ammonium sulfate ($(NH_4)_2SO_4$) and ammonium nitrate (NH_4NO_3)) play an increasingly dominant role in $PM_{2.5}$ pollution in China, especially during severe haze episodes (Huang et al., 2014; Shen et al., 2014; Tao et al., 2014). Pollutants in both acid (e.g., SO_2 and NO_x) and alkaline (e.g., NH_3) forms are crucial to the nucleation of SIA through acid-base neutralization reactions (Pan et al., 2016). These reactions increase the size and solubility of the particles, and once the bonding particles cross the threshold of diameter size (i.e., the nucleation barrier), aerosol growth becomes spontaneous (Li et al., 2016). As the most important atmospheric alkaline pollutant gas in the atmosphere, NH_3 has a significant contribution to the formation of SIA, exhibiting a base-stabilization and catalytic mechanism (Kirkby et al., 2011; Li et al., 2016).

China is the largest source of NH_3 emissions in the world, emitting over 15 Tg NH_3-N yr^{-1} in 2010, due to its low agricultural nitrogen use efficiency (NUE) in crop and livestock production (Liu et al., 2013; Gu et al., 2015). To understand the effects of NH_3 emission on $PM_{2.5}$ pollution in China, statistical analyses of measurements (Tao et al., 2014), back-trajectory receptor models (Zhang et al., 2013a), response-surface modeling techniques (Wang et al., 2011) and sensitivity simulations with atmospheric chemical transport models (Wang et al., 2014) have been widely applied. These studies usually identified a much smaller contribution of NH_3 emission to the $PM_{2.5}$ pollution compared to that of SO_2 and NO_x emissions. However, these methods generally ignore the nonlinear chemistry of aerosol formation, for instance neglecting the catalytic mechanism of NH_3 (Zhang et al., 2015) and as a consequence do not fully account for the uncertainties due to large variations in the observed $PM_{2.5}$ data (Erisman and Schaap, 2004; Liang et al., 2015). The catalytic mechanism of NH_3 may, however, be more important than the role of NH_3 as a substrate contributing to $PM_{2.5}$ formation (Kirkby et

al., 2011; Li et al., 2016). Thus, the contribution of NH_3 emission to $PM_{2.5}$ pollution in China may have been underestimated in previous studies.

The aim of this study is to re-evaluate the contribution of NH_3 ambient $PM_{2.5}$ levels. We tested the catalytic mechanism of NH_3 on $PM_{2.5}$ formation through econometric analyses across China by applying a panel model and quantile regression (see "Methods" section for details). The panel model quantifies the contribution of NH_3 emission to $PM_{2.5}$ pollution and generates unbiased estimates of the level of this contribution by eliminating confounding variables using the group deviation method (Wilke, 2011; Zhang et al., 2016). We collated monthly panel data of *in situ* $PM_{2.5}$ concentrations in 74 major cities in China from January 18 to December 31, 2013 (Fig. 1). Monthly data of pollutant emissions (SO_2, NO_x and NH_3) and meteorological factors (wind, rain, temperature, etc.) were also compiled for these cities. In addition, we obtained annual pollutant emissions, climatic factors and $PM_{2.5}$ concentration data from multiple global databases to crosscheck the results based on local monitoring. To account for the fact that $PM_{2.5}$ and its precursors can be transported from source to receptor regions over long distances, the panel model also takes wind speeds and directions into consideration. The model also includes other natural factors, such as air temperature to assess their effects.

2.Methods

2.1.Data sources.

Monthly $PM_{2.5}$ concentrations for each city were retrieved from the data center of the Ministry of Environmental Protection of China (MEPC, 2016). For the year 2013, data were available only from 18 January, when the Ministry of Environmental Protection of China began to report $PM_{2.5}$ concentration data regularly for major cities across China. The meteorological parameters, including air temperature, wind speed and direction, and precipitation, in each city were obtained from the meteorological station nearest to the monitoring site, or city centre (CMDS, 2016). If more than one meteorological station shared a similar shortest distance to the city, the average value from these meteorological stations was used.

Industrial sources accounted for 90 and 67% of the total SO_2 and NO_x emissions, respectively, in China (MEPC, 2016); thus, industrial output indicators were used to temporally distribute annual emission data over 12 months. This calculation was done applying the following equation:

$$POl_{i,a,m} = POl_{i,a} \times \frac{output_{i,m}}{\sum_{m=1}^{12} output_{i,m}} \quad (1)$$

where $POl_{i,a,m}$ is the daily emission of a pollutant of type a in month m in city i, and $POl_{i,a}$ is the annual emission of a pollutant of type a in city i; $output_{i,m}$ is the output value of industry in month m in city i.

The total monthly SO_2 and NO_x emissions in each city were significantly linearly correlated, indicating that these two pollutants share similar emission sources, in most cases large-scale fossil fuel combustion in power plants, industry and road transport (Zhang et al., 2016). Therefore, we can only select one pollutant (SO_2 **or** NO_x) or a combined pollutant (SO_2 **and** NO_x with a constant ratio) for our panel data model to avoid multicollinearity. To reflect the molar weight capacity to neutralize NH_3, we used two moles of SO_2 and one mole of NO_x as a combined pollutant for the analyses conducted in this study.

Annual grided concentration data (2001-2008) for $PM_{2.5}$ was retrieved from earth observation products provided by the National Aeronautics and Space Administration (NASA) with a resolution at 0.5×0.5° by blending total-column aerosol amount measurements from two NASA satellite instruments with information about the vertical distribution of aerosols (van Donkelaar et al., 2010; de Sherbinin et al., 2014). Matching emission data, including NH_3, NO_x, SO_2, and NMVOC were retrieved from the Emission Database for Global Atmospheric Research (EDGAR, 2016). Finally, the meteorological parameters are compiled from an updated gridded climate dataset (referred to as CRU TS3.10) based on monthly observations at meteorological stations across the world's land areas (Harris et al., 2013).

2.2.Panel data model.

Considering the multiple interactions, we designed a panel model to quantify the contributions of meteorological and anthropogenic factors to haze episodes. The panel model is set up for a comprehensive analysis of $PM_{2.5}$ formation derived from pollutant emission and meteorological factors (Zhang et al., 2016). More details of this model and its application to analyse contributions of different components to $PM_{2.5}$ formation can be found in Zhang et al (Zhang et al., 2016). The panel model incorporates data on both temporal and spatial scales simultaneously (12 months for 74 cities in this study, i.e. 884 samples in total), an approach also known as 'time-series cross-sectional data'. For example, the eastern region of the Yangtse Delta Region (YDR) illustrates how pollutant diffusion leads to a lesser impact on air pollution in Shanghai compared to other cities in the west. Thus, a simple application of cross-sectional data may underestimate the effect of pollutant emissions because emissions in Shanghai are actually much higher, while its air pollution is much lower than comparable other regions. Nevertheless, although the time-series data analysis in Shanghai can offset this underestimation, the data samples are substantially reduced if only Shanghai was to be included. Here, the panel model is capable of solving unobservable time-invariant regional differences and omitted variable problems. Moreover, $PM_{2.5}$ accumulation over previous days also affects the attribution analysis; thus, including lagged $PM_{2.5}$ pollutant concentrations as an explanatory variable is also essential. The panel model can well

capture this effect given its ability to assess both temporal and spatial variability of input data (Zhang et al., 2016). The panel model was constructed as follows in this study:

$$Y_{it} = c + Pl_{it}\beta_1 + WIND_{it}\beta_2 + \sum_j Ctrl_{itj}\beta_j + \mu_i + \varepsilon_{it} \quad (2)$$

where Y_{it} is the daily $PM_{2.5}$ concentration in month t in city i; Pl_{it} is the monthly pollutant (SO_2, NO_x and NH_3) emission; $WIND_{it}$ is the monthly average wind speed; $Ctrl_{itj}$ is a group of control variables, including air temperature, precipitation, etc., which are difficult to regulate to mitigate $PM_{2.5}$ pollution, although they are contributing factors; $\beta_1, \beta_2 \ldots \beta_j$ are the coefficients of the independent variables; c is the intercept; the effect of pollutant emission on $PM_{2.5}$ pollution is calculated as $\partial Y/\partial pl = \beta_1$; μ_i is the unobservable individual effect in city i such as the time invariant geographical situation; and ε_{it} is random error term. Contemporaneous correlation, heteroskedasticity and serial correlation are controlled to calculate asymptotically efficient parameters with Prais-Winsten regression in the statistical software package STATA12 (http://www.stata.com/stata12/) .

2.3.Quantile regression model.

Quantile regression, introduced by Koenker & Bassett (Koenker and Bassett, 1978), is a method for estimating functional relationships between variables for all portions of a probability distribution. Instead of estimating a regression model with average effects using the Ordinary Least Squares linear model, the quantile regression produces different effects along the distribution (quantiles) of the dependent variable. To obtain an estimation of a quantile regression model, we minimize the following sum of absolute residuals by linear programming methods.

$$\min_{\beta \epsilon \mathcal{R}} \sum \rho_\tau(Y_{it} - \xi(X_i, \beta)) \quad (3)$$

where Y_{it} is the average daily $PM_{2.5}$ concentration in month t in city i as above, X_i is a vector of explanatory variables, $\rho_\tau(\cdot)$ is a tilted absolute value function that yields the τth sample quantile as its solution, $\xi(X_i, \beta)$ is a parametric function with β as a vector of parameters. Quantile regression is more robust to non-normal errors and outliers than conventional least squares regression methods, and provides a more complete characterization of the data.

3.Results and Discussion

3.1.The role of NH_3 emission in $PM_{2.5}$ pollution

3.1.1.NH_3 limitation in forming SIA.

The negative coefficients of meteorological factors (i.e. wind speed, precipitation,

and air temperature) suggest a reduction of $PM_{2.5}$ concentrations with increases of these factors. In contrast, the positive coefficients of pollutant emissions on $PM_{2.5}$ concentration levels suggest the opposite (Table 1). This is consistent with existing understanding of atmospheric processes, where stronger wind dilutes pollutant concentrations, rainfall washes outs pollutants through wet deposition, and higher temperatures accelerates the decomposition of $PM_{2.5}$ (in particular through evaporation of ammonium nitrates), as well as eliminates the inversion layer that prevents dilution (Li et al., 2014; Tian et al., 2014). These findings indicate that the panel model is well able to capture and distinguish the effects from pollutant emissions and meteorological factors on $PM_{2.5}$ concentrations. To focus on the effect of pollutant emissions on $PM_{2.5}$ formation, we thus set all climatic variables as control factors and focused our discussion on the effects of pollutant emissions in the following analysis.

Here, we find that NH_3 emissions significantly affect the monthly average (mean of daily concentration) $PM_{2.5}$ concentrations across China's major cities, while at the same time the influence of SO_2 or NO_x is not significant (Table 1). Increasing NH_3 emission by 1 t km^{-2} would result in an increase of 33 μg m^{-3} of monthly average $PM_{2.5}$ concentrations, *ceteris paribus* (Table 1). In China, despite its large NH_3 emissions, the molar amount is still smaller than that of $2SO_2 + NO_x$ emissions, both calculated from our own budget studies (Gu et al., 2014, 2015) as well as resulting from analyses of global database values (i.e. EDGAR, 2016). SO_2 or NO_x emissions that do not contribute to the formation of SIA, lead to more local acidification or nutrient deposition, as is evident in the widespread occurrence of acid rain across China (MEPC, 2016). Our findings suggest that NH_3 is the critical pollutant determining the acid-base reactions related to the nucleation of $PM_{2.5}$. They further illustrate that $PM_{2.5}$ pollution in China is indeed limited by the availability of atmospheric NH_3. Similar findings have been reported in other regions, such as in Europe where regulation of NH_3 emissions has been addressed in recent years (Erisman and Schaap, 2004; Vieno et al., 2015; Backes et al., 2016). Increases in NH_3 emissions not only lead to increases in $PM_{2.5}$ concentrations due to its own mass (Ye et al., 2011; Huang et al., 2014), but also benefit the nucleation with SO_2 and NO_x emissions and facilitate the combination with other pollutants to form larger particles (Kirkby et al., 2011; Li et al., 2016).

3.1.2.Seasonal influence.

To compare the effects of NH_3, SO_2 and NO_x on the $PM_{2.5}$ levels, we separated the 12 months into two seasons: the *Major fertilization* (April to October) and *Occasional fertilization* (November to March) seasons. NH_3 emissions vary substantially between these two seasons (Huang et al., 2012), whereas SO_2 and NO_x emission are relatively stable during different months (MEPC, 2016). NH_3 emissions in the *Major fertilization* season are approximately 50% higher, while SO_2 and NO_x are only 5% higher compared to corresponding values in the *Occasional fertilization* season. We ordered all $PM_{2.5}$

concentrations in each season, then analyzed how the pollutant emissions contribute to the differences between the first (top 50% in the order) and second half (bottom 50% in the order) of $PM_{2.5}$ concentrations. By removing the effects from meteorological factors, we found that effects of NH_3 emissions on the changes of monthly average $PM_{2.5}$ concentrations between the first and second half were 5.5 and 1.5 times that of SO_2 and NO_x in the *Major fertilization* and *Occasional fertilization* seasons, respectively. In other words, NH_3 emissions have a much greater impact on the $PM_{2.5}$ pollution compared to SO_2 and NO_x in summer time and even in wintertime, when the impact of NH_3 is reduced. In winter, NH_3 emissions from cropland are much lower, because of no fertilization is taking place and the temperature is lower (Huang et al., 2012). Therefore, $PM_{2.5}$ pollution in winter is even more NH_3-limited when removing the effects from confounding factors such as temperature and wind. These findings are consistent with the results from the panel analysis discussed above and from molecular experiments reported in literature (Kirkby et al., 2011; Li et al., 2016).

3.1.3.Urban areas.

Owing to the limited transport distances of air pollutants, the distributions of acid- and alkaline-form pollutant emissions are also crucial to the $PM_{2.5}$ formation (Hu et al., 2014). Closer proximity of emission sources of different acid- and alkaline-forms pollutants facilitates the formation of secondary $PM_{2.5}$ (Gu et al., 2014; Stokstad, 2014). Hot spots of NH_3 emission largely overlap with those of SO_2 and NO_x sources in China and are mainly located in Eastern China, such as the North China Plain (NCP) and Yangtze Delta Region (YDR) (Su et al., 2011; Gu et al., 2012; Huang et al., 2012). This allows the pollutants to react more readily and form $PM_{2.5}$, contributing to a worsening air quality near or within cities in those regions. In the central areas of 74 major Chinese cities, the atmosphere is relatively NH_3-deficient, thus increasing NH_3 emission can rapidly lead to an increase in $PM_{2.5}$ concentrations (Fig. 1). Therefore, episodes of high $PM_{2.5}$ levels usually occur in cities with both a NH_3-deficient atmosphere and the occurrence of high NH_3 emissions in the immediate vicinity (e.g. intensive agricultural areas). The 10 cities with the highest $PM_{2.5}$ levels in 2013-2014 in China are all surrounded by areas with intensive agricultural production (e.g., Shijiazhuang and Zhengzhou), and no megacities without major agricultural production regions nearby are found on this list (MEPC, 2016).

Despite measures implemented for SO_2 and NO_x emissions control, air quality in China's major cities continues to deteriorate (Liang et al., 2015). In an NH_3-deficient atmosphere, the reduction of SO_2 and NO_x emissions is less efficient than that of NH_3 emission up to the point where the concentration balance shifts in a limitation from NH_3-deficient to SO_2+NO_x-deficient. In China and elsewhere, NH_3 is predominantly emitted from agriculture (Huang et al., 2012; Gu et al., 2015). Therefore, improvement of air quality in major cities will require new policies to encourage farming practices

that reduce NH_3 emission from a rapidly growing agricultural sector, especially in suburban areas and farmlands surrounding major urban areas.

3.1.4.Quantile regression.

To further capture the effect of NH_3 emissions on haze episodes in addition to their conditional means, we introduced quantile regression for four quantiles (25, 50, 75, and 90% the $PM_{2.5}$ levels) and found that NH_3, rather than SO_2 or NO_x, dominates the occurrences of $PM_{2.5}$ pollution episodes. On the one hand, the coefficients of NH_3 emissions increase in the upper quantile for both the monthly average and maximum $PM_{2.5}$ concentrations (Fig. 2), implying that NH_3 emission is significantly related to the occurrence of $PM_{2.5}$ pollution and its effect is nonlinear with a higher contribution under more severe $PM_{2.5}$ pollution. On the other hand, the coefficients of $2SO_2+NO_x$ decreased in the upper quantiles and the 90% quantile coefficient of SO_2 and NO_x is no longer significant for the monthly average $PM_{2.5}$ concentrations. For the monthly maximum $PM_{2.5}$ concentrations, the quantile coefficients of $2SO_2+NO_x$ are either not significant or negative. Such facts further suggest that $2SO_2+NO_x$ emission is not significantly correlated to the occurrence of severe $PM_{2.5}$ pollution in China, thus again supporting the fact that NH_3 substantially affected $PM_{2.5}$ pollution in China.

3.2.Periodic cycle of haze episodes

Haze episodes exhibit typical periodic cycles (Guo et al., 2014). $PM_{2.5}$ can accumulate in the atmosphere and last for several days before being dispersed or deposited to the ground by dry or wet removal processes, resulting in typical haze episodes (Guo et al., 2014). The daily average $PM_{2.5}$ concentrations are low (usually below 30 $\mu g\ m^{-3}$) in the beginning of each cycle, but can reach more than 150 $\mu g\ m^{-3}$ (maximum $PM_{2.5}$ level in each cycle, turning point) within a few days, after which the levels tend to decrease again. By counting the polluted days during clean-dirty-clean cycles, we found an average duration of 6-10 days in each periodic cycle of haze episodes across the 74 cities.

Although NH_3 emissions seem to have a dominant effect on the $PM_{2.5}$ formation compared to the influence of SO_2 and NO_x, high concentrations of both of these pollutants can lengthen the duration of each haze episode (Table 1). $PM_{2.5}$ compounds (e.g., ammonium sulfate) that combine different monomer pollutants such as SO_2 and NH_3 can stay longer in the atmosphere compared to the monomer pollutants. Therefore, the critical pollutants that determine acid-base reactions are key to the accumulation of $PM_{2.5}$ in the atmosphere. Owing to the NH_3-deficient atmosphere (relative to SO_2 and NO_x) in cities in China, the maximum $PM_{2.5}$ level in each cycle is significantly limited by NH_3 emission, but not the emission of SO_2 or NO_x (Table 1). Increasing NH_3 emission by 1 ton km^{-2} would result in an increase of 61 $\mu g\ m^{-3}$ for the maximum $PM_{2.5}$ level during each periodic cycle.

3.3.Crosschecking the role of NH_3 by alternative data sources

To crosscheck the role of NH_3 emission on $PM_{2.5}$ formation, we applied annual gridded emission data (NASA, EDGAR, CRU TS3.10) in a two-period panel model. On an annual scale, all pollutant emissions (NH_3, SO_2 and NO_x) significantly affect $PM_{2.5}$ levels (Table 2). The majority of the emission intensities of SO_2 and NO_x are in the range of 0-1×10^6 mol km^{-2} across China, substantially larger than that for NH_3 emissions, which normally range from 0 to 0.3×10^6 mol km^{-2} (Fig. 3). This illustrates as well that the emission intensities of NH_3 are spatially more evenly distributed than is the case for SO_2 and NO_x across China. A small amount of SO_2 and NO_x emissions can thus lead to an increase in $PM_{2.5}$ levels rapidly when the emission intensity is lower than 0.1×10^6 mol km^{-2} (Fig. 3a and b). However, we did not see further enhancement of $PM_{2.5}$ levels when higher emission intensities of SO_2 or NO_x occurred, especially above 0.2×10^6 mol km^{-2}. On the contrary, we found a rapid increase of $PM_{2.5}$ levels with the increase of NH_3 emssion in the majority of grid cells analysed. This reveals that $PM_{2.5}$ formation is limited by the availability of NH_3 emissions, especially especially when the SO_2 or NO_x emission intensity is high.

On this spatial scale, the higher $PM_{2.5}$ levels are also consistent with the regions with a molar ratio of $(2SO_2+NO_x)/NH_3$ greater than one (Fig. 4, Fig. 5). About 10% of gridcells do not have sufficient SO_2 and NO_x to neutralize NH_3 emissions mainly located in the rural regions including forests and grasslands in western China (Fig. 4). Therefore, we found a saturation level where NH_3 emissions do not lead to further increases of $PM_{2.5}$ levels (Fig. 3c). A few grid cells with very high NH_3 emission rates (>0.1×10^6 mol km^{-2}) would also not further increase the $PM_{2.5}$ concentrations, due to SO_2 and NO_x limitation (Fig. 4).

In fact, except in regions with intensive agriculture (including both croplands and livestock farming) but little industry or urbanization, NH_3 is usually deficient compared to the emission of acid pollutants (SO_2 and NO_x), in line with findings on the role of photochemical reactions and precursor emissions in other regions worldwide. The small mass ratios (usually rank 5-15%) of NH_3 in $PM_{2.5}$ source apportionments suggest an NH_3-deficient atmosphere at global scale (Jimenez et al., 2009; Huang et al., 2014). That means the limitation of NH_3 in severe haze formation is not only found in China, but also likely a widespread phenomenon worldwide. To assess the relevance of this potential phenomenon, we estimate the correlation between annual emission data of NH_3, SO_2, NO_x, non-methane volatile organic compounds (NMVOC) (four pollutants that are key for the formation of secondary $PM_{2.5}$ pollution, Huang et al., 2014) and $PM_{2.5}$ concentration data in each grid (0.5×0.5°) on terrestrial land areas worldwide. We used over 200 million data points in this analysis. Although we acknowledge that global inventories may be subject to large uncertainties, they are in most cases well constrained

and support analyses of large-scale pollution effects at a coarse resolution (Wang et al., 2011; Zhang et al., 2015). Correlation analysis showed that the coefficient of NH_3 emission to $PM_{2.5}$ concentrations is by far the greatest, at least twice that of the other three pollutants (Table 3). Although these statistical correlations do not identify causal relationships, they give a robust indication in relation to the effect of NH_3 emissions on $PM_{2.5}$ formation. Therefore, more focus should be directed to NH_3 mitigation not only in China, but also in other world regions with excess nitrogen inputs and resulting NH_3 emissions.

3.4.Policy implications

This paper highlights the crucial role of NH_3 in the formation of $PM_{2.5}$ pollution in China, which suggested that the future reduction of NH_3 emission should be made a priority in the Clean Air Act. Considering the substantial contribution of agricultural activities to China's NH_3 emission (Gu et al., 2015), new measures to reduce the NH_3 emission from cropland and livestock are essential, such as illustrated by the "4R" (right type, right amount, right time and right place) and better manure management in feedlots to treat and use it as fertilizer should be developed and applied to Chinese agriculture (Ju et al., 2009; Bai et al., 2014). Meanwhile, the non-agricultural NH_3 emissions from such as fossil fuel combustion is also playing an increasingly important role in $PM_{2.5}$ pollution in urban area, especially where lacks agricultural activities in the surrounding areas (Chang, 2014). Although the total amount of NH_3 emission from non-agricultural source is small (Huang et al., 2012), the concentrated dose of these NH_3 emissions and close to the SO_2 and NO_x emission sources still can result in sever air pollution in urban area (Wang et al., 2015). However, there needs to be more realization among the public and policy makers that NH_3 emissions present a serious environmental issue. For instance, the practices developed by the Task Force on Reactive Nitrogen to reduce NH_3 emission in European Union are good example for China to adapt (Backes et al., 2016). This study shows the relevance of NH_3 in the formation of secondary PM, buth also its role contributing to other effects including eutrophication, acidification, as well as a contribution to climate change and biodiversity loss (Erisman et al., 2013).

In order to allow for new technologies to be introduced, some socioeconomic barriers need to be addressed (Gu et al., 2016), such as the fragmentation of Chinese croplands under the household contract responsibility system (Zhang et al., 2013b). However, increasing the scale and structure ofagricultural operations needs follow systematic, integrated approach combining several measures, including capital investment, institutional design, educating farmers, etc. Thus, it is difficult to implement a new production system based on large scale farming in a short term. Mixed farming systems including both small and large farming operations with innovative technologies designed for application at appropriate scales may be more feasible and effective in China in the near future. Meanwhile, a healthier diet with less animal protein intake

would also reduce NH_3 emissions (Ma et al., 2013). By implementing policies to support new technologies and regulations, NH_3 emissions could be reduced by approximately 50% (Gu et al., 2015), significantly mitigating $PM_{2.5}$ pollution and at the same time benefiting food security and environmental protection objectives in China.

4.Conclusions

In this study, we found that emissions of NH_3 have a stronger association with the spatiotemporal variation of $PM_{2.5}$ levels than emissions of SO_2 and NO_x. The results derived from *in situ* monitoring data observed in major cities agreed well with the results of gridded emission data. $PM_{2.5}$ concentrations were much more strongly affected by NH_3 emssions durig severe haze episodes. Our findings suggest that NH_3 emissions, instead of the SO_2 and NO_x emissions from fossil fuel combustion as previously believed, are the key limiting factor for secondary inorganic $PM_{2.5}$ formation in urban regions of China. Therefore, we highlight the importance of reducing NH_3 emissions through improved nitrogen management from agricultural activities in mitigating $PM_{2.5}$ pollution in urban areas.

Acknowledgments

We would like to thank M. Shi for helpful comments on an earlier draft, S. Fu and Greenpeace for the $PM_{2.5}$ data support. This study was supported by the Natural Science Foundation of Zhejiang Province (No. LR15G030001, LQ14G030011) and the National Natural Science Foundation of China (Grant No. 41201502). The work contributes to the UK-China Virtual Joint Centre on Nitrogen “N-Circle” funded by the Newton Fund *via* UK BBSRC/NERC (BB/N013484/1).

References:

Backes, A.M., Aulinger, A., Bieser, J., Matthias, V., Quante, M., 2016. Ammonia emissions in Europe, part II: How ammonia emission abatement strategies affect secondary aerosols. Atmospheric Environment 126, 153-161.

Bai, Z.H., Ma, L., Qin, W., Chen, Q., Oenema, O., Zhang, F.S., 2014. Changes in Pig Production in China and Their Effects on Nitrogen and Phosphorus Use and Losses. Environmental Science & Technology 48, 12742-12749.

Chang, Y.H., 2014. Non-agricultural ammonia emissions in urban China. Atmospheric Chemistry and Physics Discussions 14, 8495-8531.

Chen, Y., Ebenstein, A., Greenstone, M., Li, H., 2013. Evidence on the impact of sustained exposure to air pollution on life expectancy from China's Huai River policy. Proceedings of the National Academy of Sciences 110, 12936-12941.

CMDS (China Meteorological Data Sharing Service System), 2016. Surface Meteorological Data. http://www.escience.gov.cn/metdata/page/index.html

de Sherbinin, A., Levy, M.A., Zell, E., Weber, S., Jaiteh, M., 2014. Using satellite data

to develop environmental indicators. Environmental Research Letters 9, 84013.
EDGAR (Emission Database for Global Atmospheric Research), 2016. Emission data. http://edgar.jrc.ec.europa.eu/
Erisman, J.W., Galloway, J.N., Seitzinger, S., Bleeker, A., Dise, N.B., Petrescu, A.M.R., 2013. Consequences of human modification of the global nitrogen cycle. Philosophical transactions of the Royal Society of London. Series B, Biological sciences 368, 20130116.
Erisman, J.W., Schaap, M., 2004. The need for ammonia abatement with respect to secondary PM reductions in Europe. Environmental Pollution 129, 159-163.
Gu, B., Fan, L., Ying, Z., Xu, Q., Luo, W., Ge, Y., Scott, S., Chang, J., 2016. Socioeconomic constraints on the technological choices in rural sewage treatment. Environmental Science and Pollution Research, doi: 10.1007/s11356-016-7267-z.
Gu, B., Ge, Y., Ren, Y., Xu, B., Luo, W., Jiang, H., Gu, B., Chang, J., 2012. Atmospheric reactive nitrogen in China: Sources, recent trends, and damage costs. Environmental Science & Technology 46, 9420-9427.
Gu, B., Ju, X., Chang, J., Ge, Y., Vitousek, P.M., 2015. Integrated reactive nitrogen budgets and future trends in China. Proceedings of the National Academy of Sciences 112, 8792-8797.
Gu, B., Sutton, M.A., Chang, J., Chang, S.X., Ge, Y., 2014. Agricultural ammonia emissions contribute to China's urban air pollution. Frontiers in Ecology and the Environment 12, 265-266.
Guo, S., Hu, M., Zamora, M.L., Peng, J., Shang, D., Zheng, J., Du, Z., Wu, Z., Shao, M., Zeng, L., Molina, M.J., Zhang, R., 2014. Elucidating severe urban haze formation in China. Proceedings of the National Academy of Sciences 111, 17373-17378.
Harris, I., Jones, P.D., Osborn, T.J., Lister, D.H., 2013. Updated high-resolution grids of monthly climatic observations - the CRU TS3.10 Dataset. International Journal of Climatology 34, 623-642.
Hu, J., Wang, Y., Ying, Q., Zhang, H., 2014. Spatial and temporal variability of $PM_{2.5}$ and PM_{10} over the North China Plain and the Yangtze River Delta, China. Atmospheric Environment 95, 598-609.
Huang, R., Zhang, Y., Bozzetti, C., Ho, K., Cao, J., Han, Y., Daellenbach, K.R., Slowik, J.G., Platt, S.M., Canonaco, F., Zotter, P., Wolf, R., Pieber, S.M., Bruns, E.A., Crippa, M., Ciarelli, G., Piazzalunga, A., Schwikowski, M., Abbaszade, G., Schnelle-Kreis, J., Zimmermann, R., An, Z., Szidat, S., Baltensperger, U., Haddad, I.E., Prévôt, A.S.H., 2014. High secondary aerosol contribution to particulate pollution during haze events in China. Nature 7521, 218-222.
Huang, X., Song, Y., Li, M., Li, J., Huo, Q., Cai, X., Zhu, T., Hu, M., Zhang, H., 2012. A high-resolution ammonia emission inventory in China. Global Biogeochemical Cycles 26, GB1030.
Jimenez, J.L., Ng, N.L., Aiken, A.C., Docherty, K.S., Ulbrich, I.M., Grieshop, A.P.ô.R., Duplissy, J., Smith, J.D., Wilson, K.R., Lanz, V.A., Canagaratna, M.R., Hueglin, C., Sun, Y.L., Tian, J., Laaksonen, A., Raatikainen, T., Rautiainen, J., Vaattovaara, P., Ehn, M., Kulmala, M., Tomlinson, J.M., Donahue, N.M., Collins, D.R., Cubison,

M.J., Dunlea, E.J., Huffman, J.A., Onasch, T.B., Alfarra, M.R., Williams, P.I., Bower, K., Kondo, Y., Schneider, J., Prevot, A.S.H., Drewnick, F., Borrmann, S., Weimer, S., Demerjian, K., Salcedo, D., Cottrell, L., Griffin, R., Takami, A., Miyoshi, T., Hatakeyama, S., Zhang, Q., Shimono, A., Sun, J.Y., Zhang, Y.M., Dzepina, K., Kimmel, J.R., Sueper, D., Jayne, J.T., Herndon, S.C., Trimborn, A.M., Williams, L.R., Kroll, J.H., Wood, E.C., Middlebrook, A.M., Kolb, C.E., Baltensperger, U., Worsnop, D.R., DeCarlo, P.F., Allan, J.D., Coe, H., 2009. Evolution of organic aerosols in the atmosphere. Science 326, 1525-1529.

Ju, X.T., Xing, G.X., Chen, X.P., Zhang, S.L., Zhang, L.J., Liu, X.J., Cui, Z.L., Yin, B., Christie, P., Zhu, Z.L., Zhang, F.S., 2009. Reducing environmental risk by improving N management in intensive Chinese agricultural systems. Proc Natl Acad Sci U S A 106, 3041-3046.

Kirkby, J., Curtius, J., Almeida, J., Dunne, E., Duplissy, J., Ehrhart, S., Franchin, A., Gagné, S., Ickes, L., Kürten, A., 2011. Role of sulphuric acid, ammonia and galactic cosmic rays in atmospheric aerosol nucleation. Nature 476, 429-433.

Koenker, R., Bassett, G., 1978. Regression Quantiles. Econometrica 46, 33-50.

Li, L., Kumar, M., Zhu, C., Zhong, J., Francisco, J.S., Zeng, X.C., 2016. Near-Barrierless Ammonium Bisulfate Formation via a Loop-Structure Promoted Proton-Transfer Mechanism on the Surface of Water. Journal of the American Chemical Society 138, 1816-1819.

Li, L., Qian, J., Ou, C.Q., Zhou, Y.X., Guo, C., Guo, Y., 2014. Spatial and temporal analysis of Air Pollution Index and its timescale-dependent relationship with meteorological factors in Guangzhou, China, 2001-2011. Environmental Pollution 190, 75-81.

Liang, X., Zou, T., Guo, B., Li, S., Zhang, H., Zhang, S., Huang, H., Chen, S.X., 2015. Assessing Beijing's PM2.5 pollution: severity, weather impact, APEC and winter heating. Proceedings of the Royal Society A: Mathematical, Physical and Engineering Science 471, 20150257.

Liu, X., Zhang, Y., Han, W., Tang, A., Shen, J., Cui, Z., Vitousek, P., Erisman, J.W., Goulding, K., Christie, P., Fangmeier, A., Zhang, F., 2013. Enhanced nitrogen deposition over China. Nature 494, 459-462.

Ma, L., Wang, F., Zhang, W., Ma, W., Velthof, G., Qin, W., Oenema, O., Zhang, F., 2013. Environmental Assessment of Management Options for Nutrient Flows in the Food Chain in China. Environmental Science & Technology 47, 7260-7268.

MEPC (Ministry of Environmental Protection of China), 2016. Data Center. http://datacenter.mep.gov.cn

Pan, Y., Tian, S., Liu, D., Fang, Y., Zhu, X., Zhang, Q., Zheng, B., Michalski, G., Wang, Y., 2016. Fossil Fuel Combustion-Related Emissions Dominate Atmospheric Ammonia Sources during Severe Haze Episodes: Evidence from ^{15}N-Stable Isotope in Size-Resolved Aerosol Ammonium. Environmental Science & Technology, doi: 10.1021/acs.est.6b00634.

Shen, G., Xue, M., Yuan, S., Zhang, J., Zhao, Q., Li, B., Wu, H., Ding, A., 2014. Chemical compositions and reconstructed light extinction coefficients of particulate

matter in a mega-city in the western Yangtze River Delta, China. Atmospheric Environment 83, 14-20.
Stokstad, E., 2014. Ammonia pollution from farming may exact hefty health costs. Science 343, 238.
Su, S., Li, B., Cui, S., Tao, S., 2011. Sulfur Dioxide Emissions from Combustion in China: From 1990 to 2007. Environmental Science & Technology 45, 8403-8410.
Tao, J., Gao, J., Zhang, L., Zhang, R., Che, H., Zhang, Z., Lin, Z., Jing, J., Cao, J., Hsu, S.C., 2014. $PM_{2.5}$ pollution in a megacity of southwest China: source apportionment and implication. Atmospheric Chemistry and Physics 14, 8679-8699.
Tian, G., Qiao, Z., Xu, X., 2014. Characteristics of particulate matter (PM10) and its relationship with meteorological factors during 2001-2012 in Beijing. Environmental Pollution 192, 266-274.
van Donkelaar, A., Martin, R.V., Brauer, M., Kahn, R., Levy, R., Verduzco, C., Villeneuve, P.J., 2010. Global Estimates of Ambient Fine Particulate Matter Concentrations from Satellite-Based Aerosol Optical Depth: Development and Application. Environmental Health Perspectives 118, 847-855.
Vieno, M., Heal, M.R., Williams, M.L., Carnell, E.J., Stedman, J.R., Reis, S., 2015. Sensitivities of UK $PM_{2.5}$ concentrations to emissions reductions. Atmospheric Chemistry and Physics Discussions 15, 20881-20910.
Wang, L.T., Wei, Z., Yang, J., Zhang, Y., Zhang, F.F., Su, J., Meng, C.C., Zhang, Q., 2014. The 2013 severe haze over southern Hebei, China: model evaluation, source apportionment, and policy implications. Atmospheric Chemistry and Physics 14, 3151-3173.
Wang, S., Nan, J., Shi, C., Fu, Q., Gao, S., Wang, D., Cui, H., Saiz-Lopez, A., Zhou, B., 2015. Atmospheric ammonia and its impacts on regional air quality over the megacity of Shanghai, China. Scientific Reports 5, 15842.
Wang, S., Xing, J., Jang, C., Zhu, Y., Fu, J.S., Hao, J., 2011. Impact Assessment of Ammonia Emissions on Inorganic Aerosols in East China Using Response Surface Modeling Technique. Environmental Science & Technology 45, 9293-9300.
Wilke, R.A., 2011. Econometric Analysis of Cross Section and Panel Data, 2nd edition. Econometrics Journal 14, B5-B9.
Ye, X., Ma, Z., Zhang, J., Du, H., Chen, J., Chen, H., Yang, X., Gao, W., Geng, F., 2011. Important role of ammonia on haze formation in Shanghai. Environmental Research Letters 6, 24019.
Zhang, F., Chen, X., Vitousek, P., 2013b. Chinese agriculture: An experiment for the world. Nature 497, 33-35.
Zhang, L., Liu, L., Zhao, Y., Gong, S., Zhang, X., Henze, D.K., Capps, S.L., Fu, T., Zhang, Q., Wang, Y., 2015. Source attribution of particulate matter pollution over North China with the adjoint method. Environmental Research Letters 10, 84011.
Zhang, R., 2010. Getting to the Critical Nucleus of Aerosol Formation. Science 328, 1366-1367.
Zhang, R., Jing, J., Tao, J., Hsu, S.C., Wang, G., Cao, J., Lee, C.S.L., Zhu, L., Chen, Z.,

582 Zhao, Y., Shen, Z., 2013a. Chemical characterization and source apportionment of
583 $PM_{2.5}$ in Beijing: seasonal perspective. Atmospheric Chemistry and Physics 13,
584 7053-7074.
585 Zhang, X., Wu, Y., Gu, B., 2016. Characterization of haze episodes and factors
586 contributing to their formation using a panel model. Chemosphere 149, 320-327.
587 Zhang, Y., Cao, F., 2015. Fine particulate matter ($PM_{2.5}$) in China at a city level.
588 Scientific Reports 5, 14884.
589
590

591 **Table 1**. Estimated coefficients in a panel model with monthly data

	Average $PM_{2.5}$ (μg m^{-3})	Maximum $PM_{2.5}$ (μg m^{-3})	Duration of a haze episode (day)
$2SO_2+NO_x$ (10^6 mol km^{-2})	388.1	700.1	73.72***
	(265.8)	(622.1)	(27.62)
NH_3 (10^6 mol km^{-2})	560.9***	1036.4***	110.8***
	(147.3)	(387.8)	(14.96)
Precipitation (mm)	-1.501***	-2.621***	-0.108**
	(0.204)	(0.732)	(0.0465)
Wind speed (m s^{-1})	-25.00***	-41.24***	-0.952***
	(2.736)	(6.320)	(0.227)
MMT (°C)	-2.531***	-3.115***	-0.0189
	(0.130)	(0.482)	(0.0118)
N	884	547	547
within R^2	0.645	0.384	0.094
F stat	142.56	33.48	14.40
Hausman test	13.69	29.39	63.34

592 Note that the coefficient represents how much the $PM_{2.5}$ concentrations or duration of a
593 haze episode change when increasing one unit of influencing factors in the panel model.
594 Data in brackets represent the standard errors. Average $PM_{2.5}$ refers to the mean of
595 $PM_{2.5}$ concentration in a month in each city. Maximum $PM_{2.5}$ refers to the mean of the
596 maximum $PM_{2.5}$ concentration in each periodic cycle of haze episode. Periodic cycles of
597 haze episode refers to the times of haze episode occurred in a month. SO_2 & NO_x refers
598 to the emission intensity of SO_2 and NO_x in a city. MMT refers to mean monthly
599 temperature. Fixed effect panel model is applied in this analysis owing to the large
600 value of Chi2 in Huasman test. Standard errors in parentheses. * $p < 0.10$, ** $p < 0.05$,
601 *** $p < 0.01$.
602
603

Table 2 Estimated coefficients in a two-period panel model with annual data

	Coefficient	Standard error	t	P>t
NH_3 (10^6 mol km^{-2})	77.439	4.781	16.200	0.000
SO_2 (10^6 mol km^{-2})	2.310	0.663	3.480	0.001
NO_x (10^6 mol km^{-2})	1.949	0.988	1.970	0.049
Wind speed (m s^{-1})	3.300	0.253	13.030	0.000
Precipitation (mm)	-0.004	0.000	-8.130	0.000
MAT (°C)	-0.057	0.079	-0.730	0.468
N	7492			
Within R^2	0.2109			
F stat	117.83			
Hausman test	868.30			

Note, mean value of first and last three years of data available are selected as two periods, i.e., mean value of pollutant emissions and climatic factors on $PM_{2.5}$ from 2001 to 2003 and 2006 to 2008 for the whole China are used. MAT refers to mean annual temperature. Fixed effect panel model is applied in this analysis owing to the large value of Chi2 in Huasman test. Standard errors in parentheses. * $p < 0.10$, ** $p < 0.05$, *** $p < 0.01$.

613 **Table 3** Coefficients of correlation among $PM_{2.5}$, SO_2, NO_x, NMVOC and NH_3 on the
614 global scale with 0.5×0.5° grid data

	$PM_{2.5}$	SO_2	NO_x	NMVOC	NH_3
$PM_{2.5}$	1				
SO_2	0.4342	1			
NO_x	0.4497	0.6499	1		
NMVOC	0.4607	0.6416	**0.9796**	1	
NH_3	**0.6475**	0.4990	0.5679	0.5699	1

615
616
617

Figure legend

Figure 1 Locations of these 74 cities and their average and maximum $PM_{2.5}$ level in 2013. The background color refers to the NH_3 emission intensity on the provincial scale.

Figure 2 Coefficients of quantile regressions of emissions of NH_3 and SO_2&NO_x to the $PM_{2.5}$ level under different quantile. (a) Average monthly $PM_{2.5}$ concentration; (b) Average of the maximum $PM_{2.5}$ concentration in each period cycle.

Figure 3 Correlations of pollutant emissions and $PM_{2.5}$ level by using grid data in 2008 across China. (a) SO_2; (b) NO_x; (c) NH_3; (d) $2SO_2+NO_x$

Figure 4 Molar ratios of emissions of SO_2 and NO_x to NH_3 in 2008. The tope one refers to the molar ratio of acid pollutants to NH_3, and > 1 of the ratio represents NH_3 limitation to the $PM_{2.5}$ pollution. The bottom one refers to the molar ratio of SO_2 to NH_3, and > 1 of the ratio represents the pollution reach ammonium nitrate equilibrium. One mole of SO_2 can react with two moles of NH_3, thus $2SO_2$ is used to indicate the limitation of $PM_{2.5}$ pollution related to different forms of pollutant emission.

Figure 5 Changes of $PM_{2.5}$ pollution and pollutant emissions from 2001 to 2008. The left and middle four figures used the average data from 2001 to 2003, and 2006 to 2008, respectively, and the right four figures were the difference between the left and middle four figures.

643

644 **Figure 1**

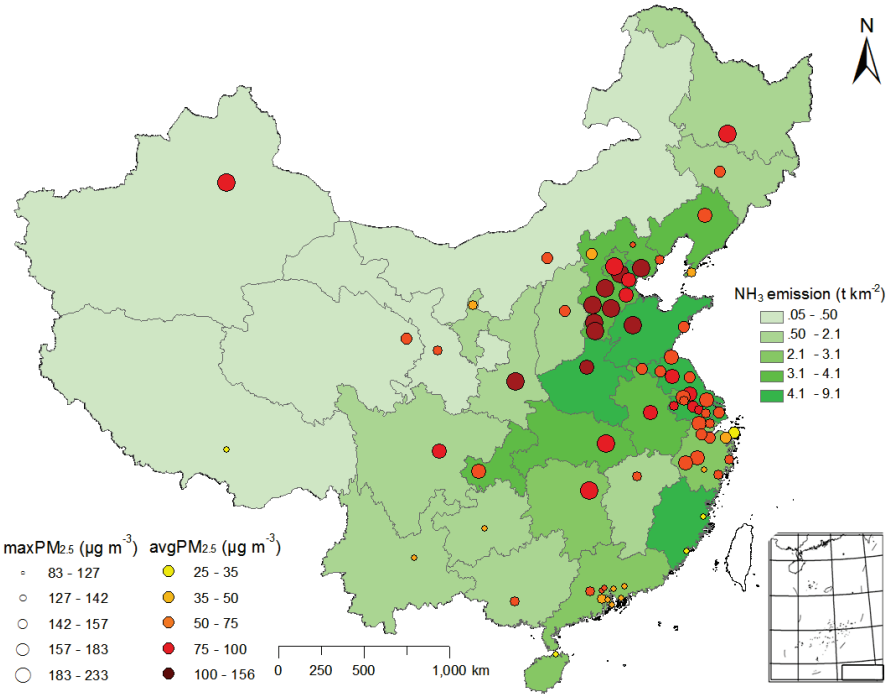

645

646

647

648 **Figure 2**

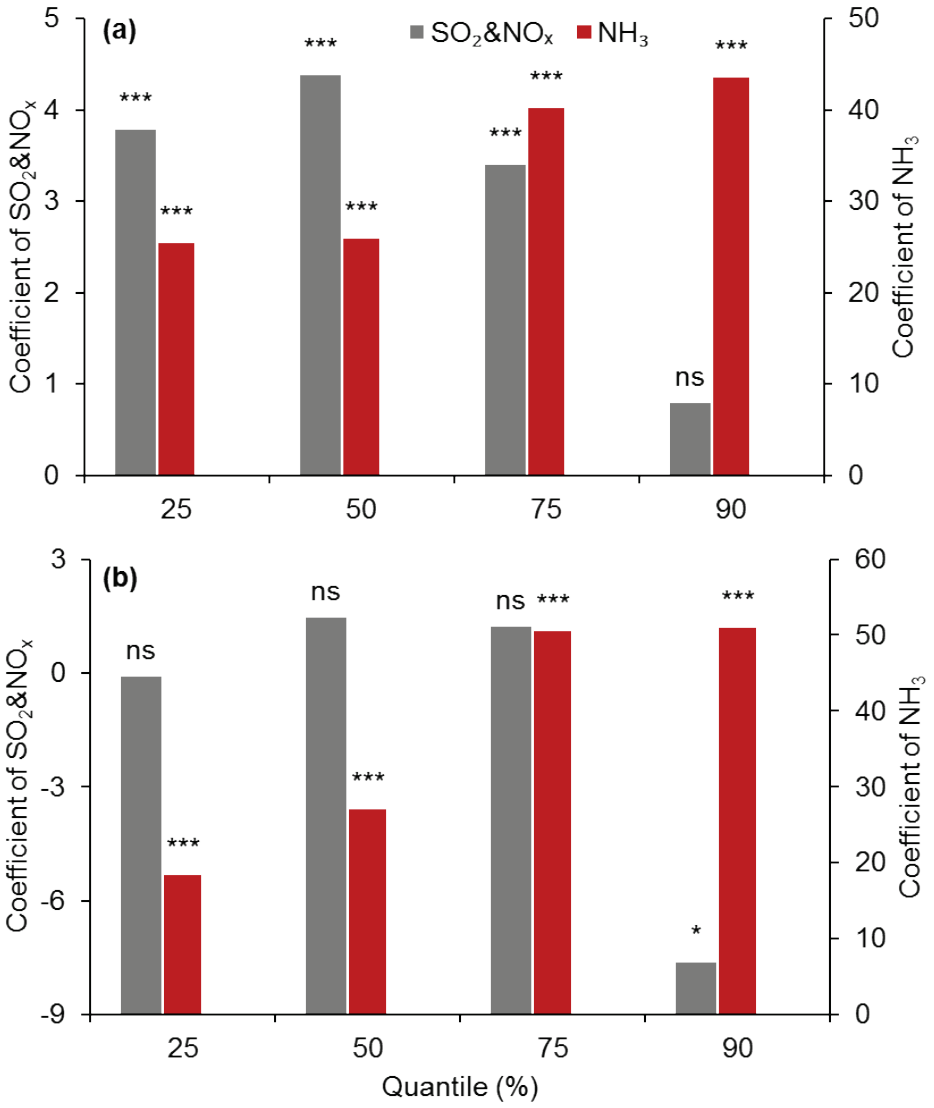

649

650

651 **Figure 3**

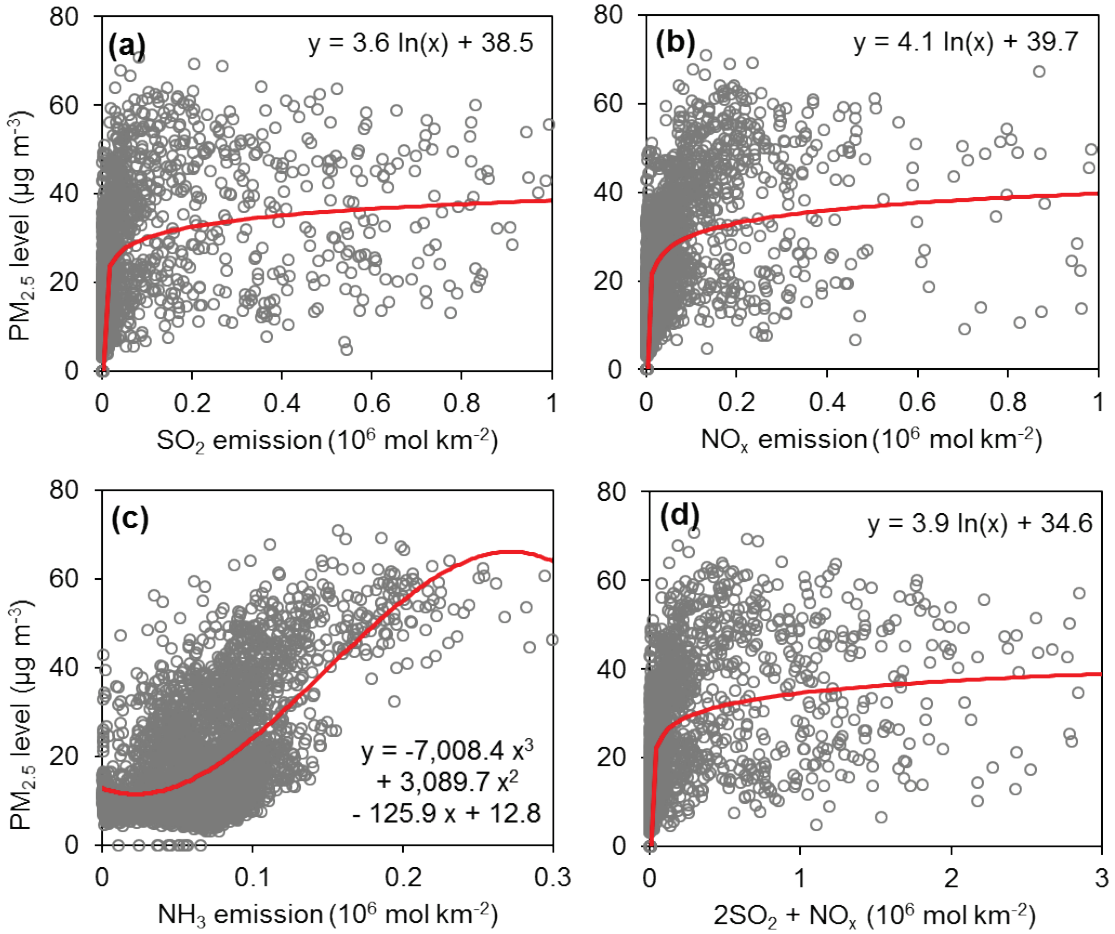

652

653

Figure 4

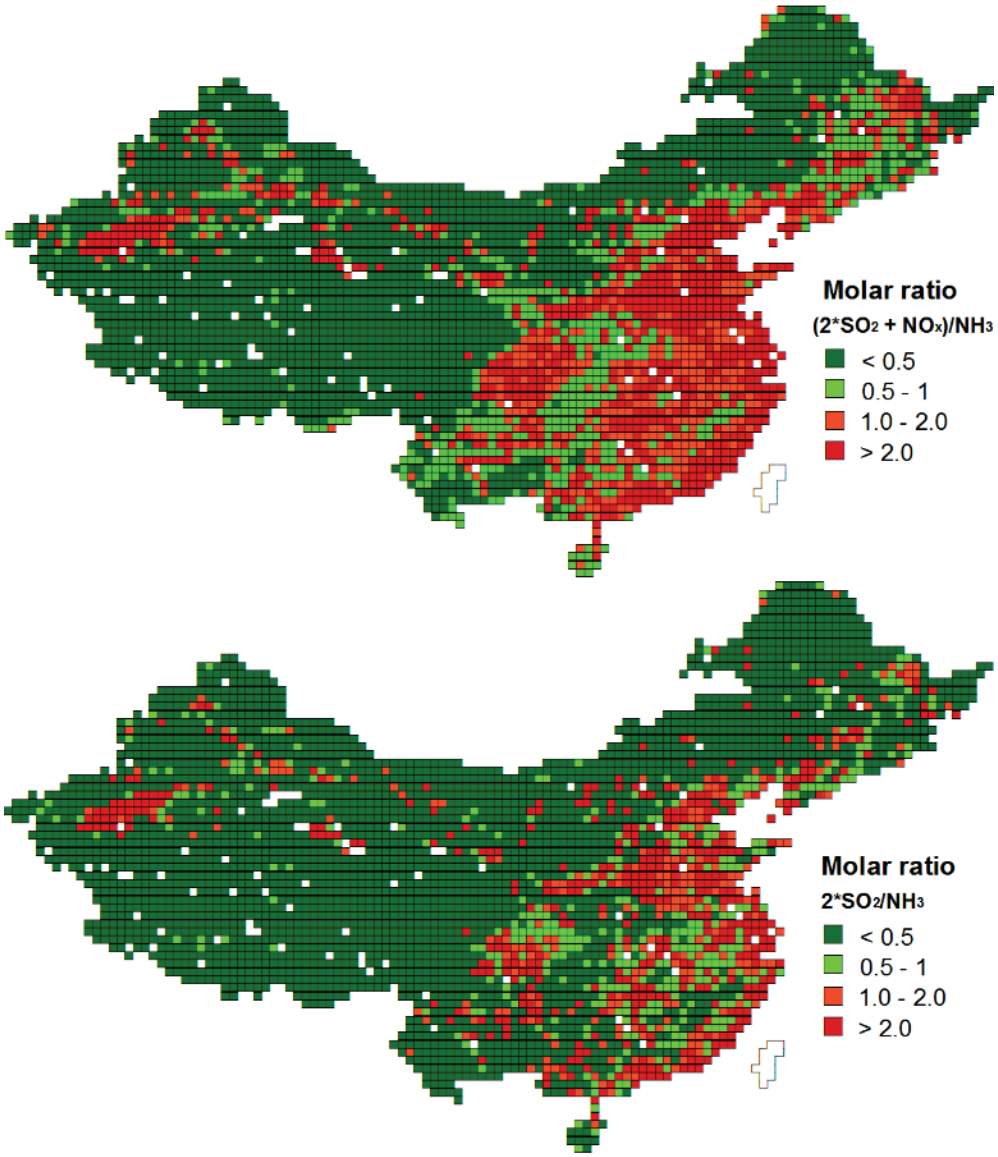
Molar ratio
(2*SO2 + NOx)/NH3
< 0.5
0.5 - 1
1.0 - 2.0
> 2.0
Molar ratio
2*SO2/NH3
< 0.5
0.5 - 1
1.0 - 2.0
> 2.0

Figure 5

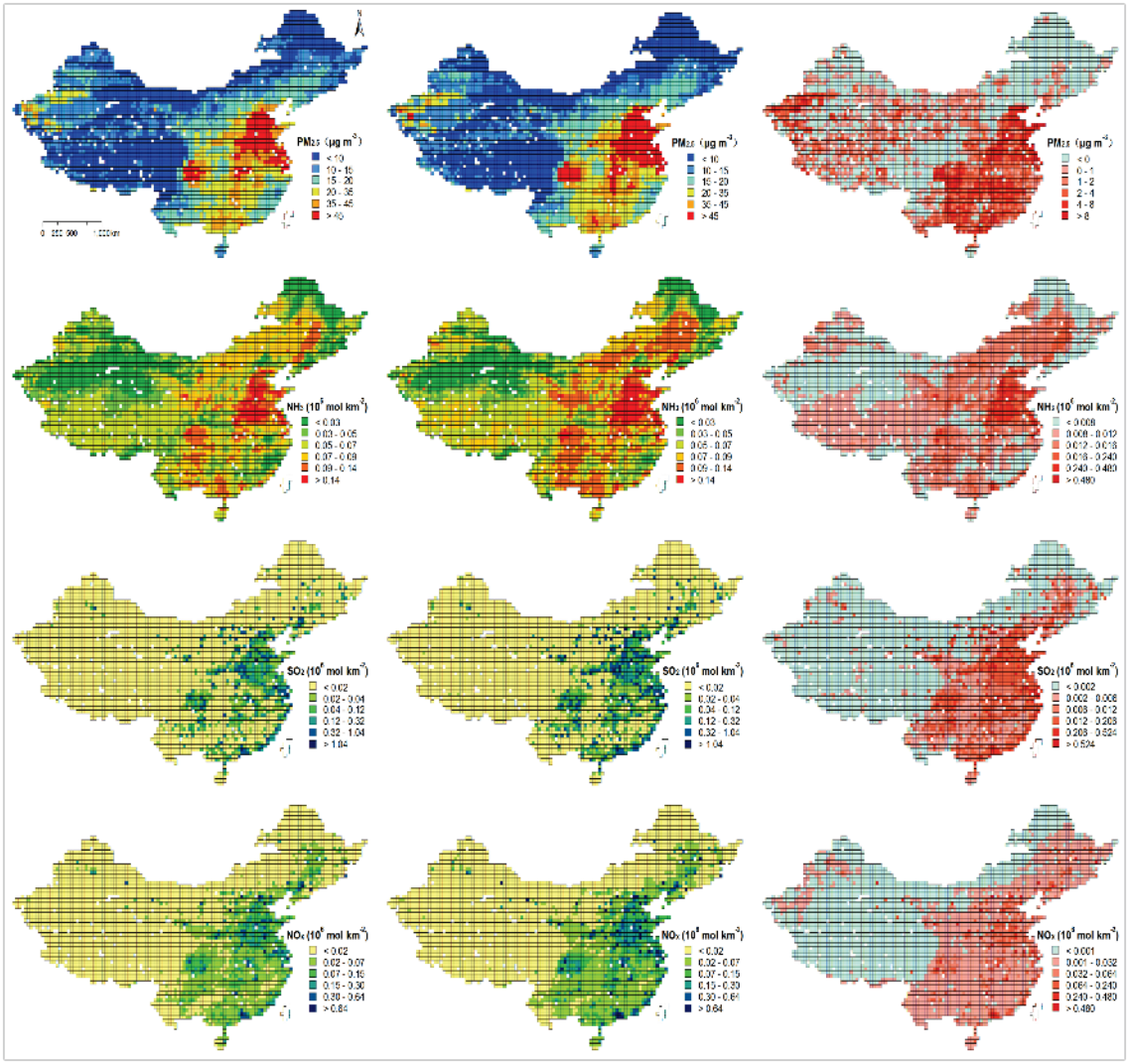
PM2.5 (μg m-3)
< 10
10 - 15
15 - 20
20 - 35
35 - 45
> 45
PM2.5 (μg m-3)
< 10
10 - 15
15 - 20
20 - 35
35 - 45
> 45
PM2.5 (μg m-3)
< 0
0 - 1
1 - 2
2 - 4
4 - 8
> 8
NH3 (10^6 mol km-2)
< 0.03
0.03 - 0.05
0.05 - 0.07
0.07 - 0.09
0.09 - 0.14
> 0.14
NH3 (10^6 mol km-2)
< 0.03
0.03 - 0.05
0.05 - 0.07
0.07 - 0.09
0.09 - 0.14
> 0.14
NH3 (10^6 mol km-2)
< 0.008
0.008 - 0.012
0.012 - 0.018
0.018 - 0.240
0.240 - 0.480
> 0.480
SO2 (10^6 mol km-2)
< 0.02
0.02 - 0.04
0.04 - 0.12
0.12 - 0.32
0.32 - 1.04
> 1.04
SO2 (10^6 mol km-2)
< 0.02
0.02 - 0.04
0.04 - 0.12
0.12 - 0.32
0.32 - 1.04
> 1.04
SO2 (10^6 mol km-2)
< 0.002
0.002 - 0.008
0.008 - 0.012
0.012 - 0.208
0.208 - 0.524
> 0.524
NOx (10^6 mol km-2)
< 0.02
0.02 - 0.07
0.07 - 0.15
0.15 - 0.30
0.30 - 0.64
> 0.64
NOx (10^6 mol km-2)
< 0.02
0.02 - 0.07
0.07 - 0.15
0.15 - 0.30
0.30 - 0.64
> 0.64
NOx (10^6 mol km-2)
< 0.001
0.001 - 0.032
0.032 - 0.064
0.064 - 0.240
0.240 - 0.480
> 0.480